PAIN® 155 (2014) 1861–1870

www.elsevier.com/locate/pain

Human sensory neurons: Membrane properties and sensitization by inflammatory mediators

Steve Davidson [a,1], Bryan A. Copits [a,1], Jingming Zhang [b], Guy Page [b], Andrea Ghetti [b], Robert W. Gereau IV [a,*]

[a] Washington University Pain Center and Department of Anesthesiology, Washington University School of Medicine, St Louis, MO 63110, USA
[b] AnaBios Corporation, San Diego, CA 92109, USA

Sponsorships or competing interests that may be relevant to content are disclosed at the end of this article.

ARTICLE INFO

Article history:
Received 25 April 2014
Received in revised form 28 May 2014
Accepted 20 June 2014

Keywords:
Bradykinin
Dorsal root ganglia
Human
Itch
Nociception
Pain
Sensitization

ABSTRACT

Biological differences in sensory processing between human and model organisms may present significant obstacles to translational approaches in treating chronic pain. To better understand the physiology of human sensory neurons, we performed whole-cell patch-clamp recordings from 141 human dorsal root ganglion (hDRG) neurons from 5 young adult donors without chronic pain. Nearly all small-diameter hDRG neurons (<50 μm) displayed an inflection on the descending slope of the action potential, a defining feature of rodent nociceptive neurons. A high proportion of hDRG neurons were responsive to the algogens allyl isothiocyanate (AITC) and ATP, as well as the pruritogens histamine and chloroquine. We show that a subset of hDRG neurons responded to the inflammatory compounds bradykinin and prostaglandin E_2 with action potential discharge and show evidence of sensitization including lower rheobase. Compared to electrically evoked action potentials, chemically induced action potentials were triggered from less depolarized thresholds and showed distinct afterhyperpolarization kinetics. These data indicate that most small/medium hDRG neurons can be classified as nociceptors, that they respond directly to compounds that produce pain and itch, and that they can be activated and sensitized by inflammatory mediators. The use of hDRG neurons as preclinical vehicles for target validation is discussed.

1. Introduction

Cultures of rodent dorsal root ganglion (rDRG) neurons are useful for studying the molecular and cellular mechanisms underlying sensory transduction of painful stimuli, but notable translational failures have raised questions about the wisdom of developing drugs for pain relief in rodents for eventual use in humans [34,53]. Biological differences between rodent and human physiology may present significant obstacles to translation, but are rarely considered [32,38,42,51]. One strategy to minimize this risk is to confirm observations made in rodents directly in viable human sensory neurons. However, obtaining healthy hDRG from adult donors has been a limiting factor. Instead, sensory neurons retrieved primarily from ganglionectomized chronic pain patients or fetuses have been studied [1,6,7,31,37,41,49]. Consequently, little is known about membrane properties and chemosensitivity of adult hDRG neurons from individuals without chronic pain.

Increasing evidence suggests that the repertoire of channels, receptors, and signaling molecules expressed in hDRG differ critically from those of model organisms, and even homologous proteins can exhibit altered ligand binding affinities, functional properties, and accessory protein interactions. For example, voltage-gated sodium channels produce a unique tetrodotoxin-resistant current in hDRG neurons not previously identified in rodents [18]. Additionally, $GABA_A$ receptor–evoked currents in rodent DRG are effectively blocked by picrotoxin and bicuculline, but neither antagonist blocked GABAR currents from hDRG neurons, suggesting fundamental functional differences in human sensory neurons [50]. Genetic differences of homologous receptors between human and model organisms have also been identified. For instance, mouse DRG express a large family of more than 30 genes encoding mas-related G-protein-coupled receptors (Mrgprs), several of which

* Corresponding author. Address: Department of Anesthesiology, Pain Center, Washington University School of Medicine, 660 South Euclid Ave, Campus Box 8054, Saint Louis, MO 63110, USA. Tel.: +1 (314) 362 8312; fax: +1 (314) 362 8334.
E-mail address: gereaur@wusm.wustl.edu (R.W. Gereau IV).
[1] The first 2 authors contributed equally to this article, and both should be considered first author.

http://dx.doi.org/10.1016/j.pain.2014.06.017
0304-3959/

are involved in nociception and pruriception, compared with only 4 types of Mrgprs in human [20,30,56]. These observations of critical variations in protein expression and function between rodent and hDRG neurons may render physiological mechanisms identified in rodent as invalid targets for therapeutic studies aimed at humans. To enhance target validation and translational potential of novel analgesics, these variations must be identified and functionally characterized. Currently, scant evidence exists on the sensitivity of hDRG neurons to directly applied chemical stimuli used in studies of rodent nociceptors.

Sensitization of primary afferent neurons is thought to be a major contributor to ongoing pain, and compounds that block or reverse sensitization are attractive targets for analgesic drug development [5,55]. Rodent studies support the concept that blocking the signal initiated by mediators of sensitization reduces neural hyperexcitability and nocifensive behaviors [9]. However, little is known about whether inflammatory mediators directly sensitize or activate human sensory neurons.

Here, we establish the electrophysiological profile of hDRG neurons from 5 donors without chronic pain. A high proportion of tested neurons responded to the chemical algogens AITC and ATP, as well as to the itch-producing compounds histamine and chloroquine. We also show that human sensory neurons can be sensitized by the inflammatory mediators bradykinin and PGE_2. Our results take an important step toward closing the translational gap between studies in model organisms and effective therapeutic development in humans.

2. Methods

2.1. Donors

Human DRGs were isolated from U.S. organ donors (mean age 18.2 years) with full legal consent for use of tissue for research (Table 1).

2.2. DRG preparation

DRGs from the second thoracic vertebra (T2) through the 12th thoracic vertebra (T12) were used in the present study. The DRGs were dissected to remove all connective tissue and fat. Subsequently, the ganglia were enzymatically digested at 37°C for 2 h using AnaBios' proprietary enzyme mixture. Samples were then centrifuged for 2 min at 200×*g*, solution was gently removed, and tissue was washed 3 times, followed by resuspension in DMEM/F12 (Lonza; Allendale, NJ) containing 1% horse serum (Thermo Fisher Scientific; Rockford, IL). Ganglia were mechanically dissociated by gentle trituration through the fire-polished tip of a sterile glass Pasteur pipette. Dissociated cells were seeded on glass coverslips that had been precoated with poly-D-lysine. Cells were maintained in culture at 37°C with 5% CO_2 in DMEM/F12 supplemented with 10% horse serum (Thermo Fisher Scientific), 2 mM glutamine, 25 ng/mL hNGF (Cell Signaling Technology, Danvers, MA), 25 ng/mL GDNF (Peprotech, Rocky Hill, NJ), and penicillin/streptomycin (Thermo Fisher Scientific). Half of the culture media was replaced with fresh media every 3 days.

2.3. Electrophysiological recordings

Human DRG neurons were incubated in culture at least 3 days before recording. This time was necessary to allow satellite glial cells surrounding the soma to move down onto the coverslip, thus exposing the plasma membrane to permit pipette access and subsequent formation of a tight seal. During the course of preliminary experiments, it was determined that aggressive enzymatic cell dissociation could provide DRG neurons completely stripped of satellite glial cells. While these preparations provided immediate access to patch clamp–based electrophysiology recordings, those treatments appeared to compromise cell health (depolarized $V_m < -40$ mV and survival in culture <24 h). Cells exhibited a wide range of diameters, and both small and large neurons were healthy and patchable; however, we chose to focus on smaller cells as presumptive nociceptive neurons for this study. Neurons that exhibited a resting membrane potential more depolarized than −40 mV were considered unhealthy and were not analyzed.

Whole-cell recordings were made in current clamp using pipettes pulled from thick-walled borosilicate glass (Warner Instruments; Hamden, NJ), with open tip resistances ranging from 2 to 4 MΩ using a P-97 horizontal puller (Sutter Instrument; Novato, CA). The extracellular solution contained (in mM): 145 NaCl, 3 KCl, 2.5 $CaCl_2$, 1.2 $MgCl_2$, 10 HEPES, 7 glucose, adjusted to pH 7.4 with NaOH, and was warmed to 32°C. The intracellular solution contained (in mM): 130 K-gluconate, 5 KCl, 5 NaCl, 3 Mg-ATP, 0.3 EGTA, 10 HEPES, adjusted to pH 7.3 with KOH and 294 mOsm using sucrose. Following gigaseal formation, it was often necessary to combine a 300 to 500 mV zap pulse with negative pressure to achieve whole-cell configuration in these cells. After whole-cell access and nulling the slow transients with the capacitance-compensation circuit of the amplifier, cells were dialyzed for a minimum of 2 min while holding at −60 mV. Neurons were recorded using Patchmaster software (Heka Instruments; Bellmore, NY) controlling an EPC10 USB amplifier (Heka). Data were sampled at 20 kHz and analyzed off-line.

All recordings were performed with continuous whole-bath perfusion. Gravity-fed solution flow and exchange were controlled with a 16-channel valve controller (PC-16, Bioscience Tools), and flow rates were ~1 to 2 mL/min. This resulted in a void time of 15 to 20 s between the time solutions were switched and when they first entered the bath. The temperature was maintained at 32°C with a heated chamber stage (TC-E35, Bioscience Tools), controlled using a 2-channel bipolar temperature controller (TC2-80-150, Bioscience Tools) and monitored constantly with a feedback thermistor positioned in the bath.

Chemicals (Sigma Aldrich, St. Louis, MO) bradykinin (100 nM), PGE_2 (1 μM), AITC (30 μM), ATP (100 μM), histamine (100 μM), and chloroquine (100 μM) were prepared in external solution.

2.4. Analysis and statistics

All recordings were performed within 9 days of dissociation; over this period, hDRG neurons did not exhibit any differences in cell size, whole-cell capacitance, or membrane excitability, indicating biophysical stability over the duration of the experiments.

Table 1
Donor information.

Donor no.	Age, y	Sex	BMI, kg/m^2	Ethnicity	Cause of death	Neurons recorded
1	21	Male	22.9	White	Anoxia	38
2	13	Male	20.0	White	Head trauma	36
3	19	Male	26.9	Asian	Head trauma	38
4	19	Female	26.1	White	Stroke	21
5	19	Male	25.3	Hispanic	Stroke	8

BMI, body mass index.

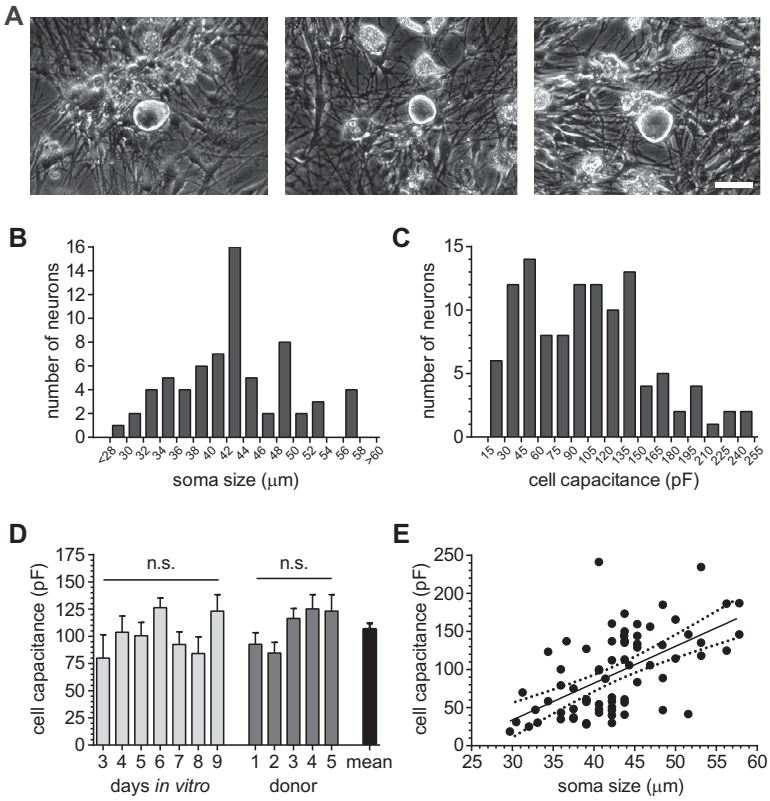

Fig. 1. Physical characteristics and capacitance of hDRG neurons. (A) Phase-contrast images depicting dissociated hDRG neurons illustrating neurons that are suitable for patch-clamp recordings. Scale bar = 50 μm. (B) Histogram summarizing the range of hDRG soma diameters from a subset of recorded neurons. Diameters were determined using a calibrated ocular eyepiece. (C) Histogram of whole-cell capacitance from recorded hDRG neurons. (D) Summary graph of the whole-cell capacitance from all donors and across time in vitro. Number of neurons indicated in parentheses: 3 DIV (6), 4 DIV (21), 5 DIV (16), 6 DIV (35), 7 DIV (21), 8 DIV (11), 9 DIV (19). n.s., not significantly different. (E) Plot of whole-cell capacitance vs soma diameter indicating a linear relationship between these 2 measurements. $R^2 = 0.336$; $Y = 4.84x + 23.0$ ($P < .0001$). Dotted lines represent 95% confidence interval.

Additionally, numerous biophysical properties including resting membrane potential, action potential (AP) amplitude, and rheobase between the 5 donors examined showed no differences. The recordings were therefore pooled across donors and days in vitro for analyses of action potential waveforms and measures of sensitization.

Membrane properties were calculated using several protocols in current clamp mode. Input resistance was determined with a hyperpolarizing current injection of 50 to 100 pA. Action potentials were elicited by a series of either 800 ms step current injections or during a 500 ms ramp, and increased by 50 to 100 pA per sweep until cells reached threshold. Intersweep intervals were 3 to 5 s. Chemical applications were monitored in gap-free recording mode.

Data were analyzed off-line with Igor Pro (WaveMetrics, Portland, OR) using custom-written macros and the NeuroMatic plug-in (v2.00). Data organization and statistical analysis were performed by Microsoft Excel and Prism 5 (GraphPad, La Jolla, CA). Linear regression was performed to determine covariation. One-way ANOVA was used to determine differences in multiple groups. Student's *t* test was used to test for significance between 2 groups, except for bradykinin-treated cells, where paired *t* tests were used to compare neurons before and after chemical application. All data are presented as mean ± standard error of the mean.

3. Results

3.1. Physical appearance and capacitance of human DRG neurons in vitro

Whole-cell patch clamp recordings were performed in vitro over a range of 7 days on 141 hDRG neurons from 5 donors. Examples of hDRG neurons isolated in culture are shown in Fig. 1A. Neuronal membranes generally appeared clear in bright-field illumination, with a subset of cells exhibiting brown lipofuscin deposits in the membranes surrounding the nucleus. The mean diameter measured from a representative subset of recorded neurons was 42.8 ± 0.8 μm (Fig. 1B, $n = 69$). A population of cells was observed in culture with diameters over 60 μm, but we chose to focus on small- to medium-size cells, which are more likely to represent the slower-conducting Aδ- and C-fiber nociceptors. After break-in, whole-cell capacitance ranged from 16.8 to 248.9 pF, with an average of 106.3 ± 5.1 pF (Fig. 1C, $n = 118$). Neither the mean diameter nor whole-cell capacitance differed between donors or days in vitro, indicating consistency between individuals and repeatability for the isolation and culturing techniques (Fig. 1D). A weak linear correlation was found between whole-cell capacitance and soma diameter, suggesting that while capacitance scales with diameter in human neurons, nonspherical soma morphology or process growth may limit our accuracy in assessing the degree of correlation (Fig. 1E).

3.2. Action potential parameters from naïve hDRG neurons

Naïve hDRG neurons had a resting membrane potential of −62.4 ± 2.0 mV ($n = 133$), which did not differ across days in culture or by donor (Fig. 2C). To investigate hDRG excitability, action potentials (APs) were evoked with current injections using both a ramp and a step protocol. Most neurons fired only a single spike to current injection; when multiple action potentials were evoked, analyses were performed on the first spike (Fig. 2A). To calculate the voltage threshold of activation, the first derivative of the action

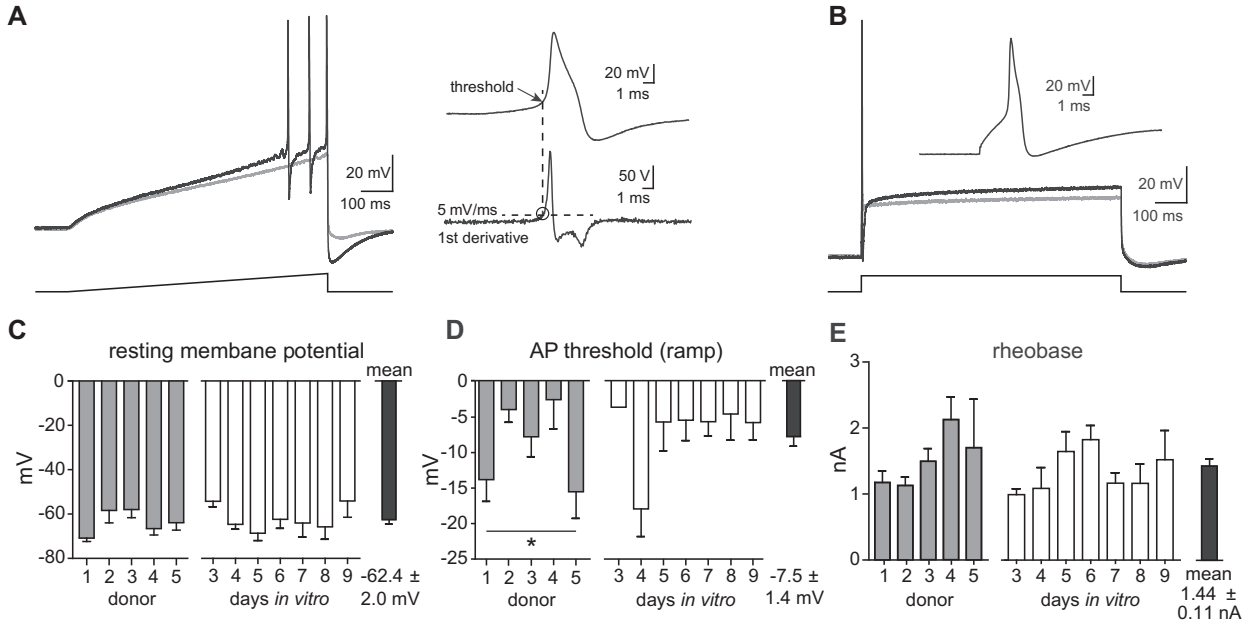

Fig. 2. Excitability of hDRG neurons. (A) Action potentials evoked by a 500 ms ramp current injection protocol. Gray trace depicts membrane voltage during a subthreshold step, with the subsequent sweep in the series of increasing current injections eliciting action potentials (black trace). Current steps were increased 50 to 100 pA per sweep. AP threshold was taken as the membrane voltage at the point in which the fist derivative waveform of the first action potential crossed 5 volts/s (dashed line). (B) Rheobase was established from an 800 ms step current protocol, increased in 50 to 100 pA increments. The gray trace illustrates a subthreshold depolarization, with the following sweep eliciting an action potential at the start. A majority of hDRG (70%) fired an action potential during the initial rising step of the current injection. (C) Summary graph of the resting membrane potential across donors and time in culture, which was not significantly different. (D) Summary of the action potential threshold across donors and time in culture, determined by ramp current injections shown in (A). Action potential thresholds were variable by donor (*$P < .05$, 1-way ANOVA), although no post hoc comparisons between any groups were significant (Tukey's multiple comparison test). Threshold did not differ by days in vitro. (E) Graph of rheobase (step current thresholds to elicit an AP), which did not differ by donor or days in vitro.

potential waveform was plotted, and the value at which the rate of voltage change exceeded 5 volts/s was taken as the threshold (Fig. 2A, inset). Overall, action potential threshold varied from donor to donor (1-way ANOVA, $P < .05$); however, no pairwise comparisons between donors were significantly different from one another (Tukey's multiple comparison test). Over the course of 7 days in vitro, no significant differences in action potential threshold were observed (Fig. 2D). Rheobase, the step current required to evoked an action potential, was 1.44 ± 0.11 nA ($n = 110$) and did not vary from donor to donor or across days in vitro (Fig. 2B, E). The mean action potential peak amplitude (from 0 mV) was 64.6 ± 0.9 mV and did not differ between donors or with extended time in culture. Additional features of naïve hDRG membrane properties are documented in Table 3. These data show little variability in parameters of membrane excitability between donors and preparations, and they indicated that hDRG neurons remain stable across several days in vitro.

3.3. Action potential "shoulder" of hDRG neurons

Further inspection of hDRG action potentials showed that 97% (73 of 75) of recorded cells exhibited a "shoulder" on the falling phase of the action potential. Representative examples of action potentials with a large and small shoulder are shown (Fig. 3A, insets). The change in voltage with respect to time is indicated in phase-plane plots, which illustrate the distinct components of the action potential, including the rapidly accelerating/decelerating rising phase and the slower, dynamic, falling phase, which includes the shoulder (Fig. 3A, shaded). We were curious whether shoulder size was indicative of any specific cellular signatures, and used the first derivative of the action potential waveform to establish shoulder onset and offset times (the inflection point on either side of the shoulder peak). Shoulder size was plotted on a frequency histogram (Fig. 3B). Shoulder areas exhibited a range of values from 0 to 186 mV·ms with a mean of 41.6 ± 3.7 mV·ms ($n = 75$). No significant correlation was detected between shoulder size and the mean slope of the rising phase, or the maximum and minimum rates of change in membrane voltage over time (data not shown). We also did not find a significant correlation between shoulder size and measurements of physical cell size or excitability (Fig. 3C).

3.4. Afterhyperpolarization kinetics of hDRG action potentials

After the shoulder, hDRG neurons exhibited an afterhyperpolarization (AHP), a component of the action potential that could act as a modulator of interspike intervals and firing frequency. We noticed that these AHP decays exhibited a wide range of durations. To quantify this, we calculated the mean weighted tau values from single or double exponential fits of the voltage decay. Examples of a range of fast and slower waveforms are shown in Fig. 4A. The mean amplitude and tau values for naïve hDRG neurons are listed in Table 3. Tau values ranged from 2.8 to 88 ms and AHP kinetics for each cell are shown in a frequency histogram (Fig. 4B). Tau values strongly correlated with action potential width (measured across the AP from a 5 mV/ms threshold), but they did not correlate with cell capacitance or action potential peak (Fig. 4C, D; AP peak data not shown). These data demonstrate that hDRGs exhibit a wide range of AHP kinetics, which may impart unique firing characteristics to individual neurons.

3.5. Activation of hDRG by chemical algogens and pruritogens

Ganglionectomized hDRG neurons from pain patients have been shown to respond to the algogens capsaicin and acidic pH [3,6,7], but the effects of many commonly used algogens in rodent

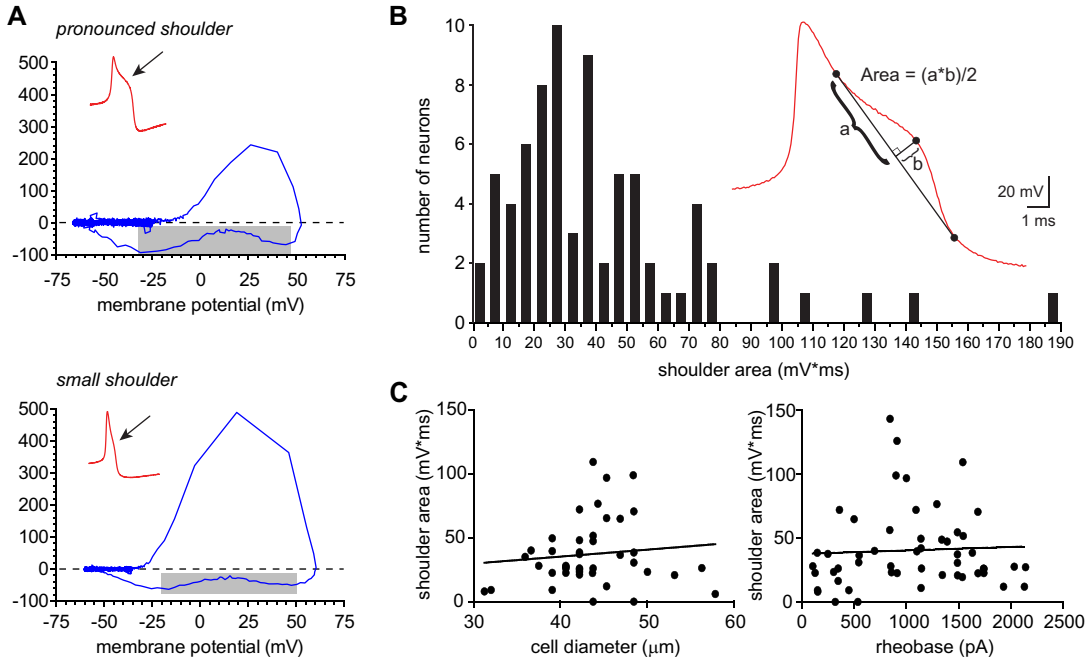

Fig. 3. Waveform and shoulder analysis of hDRG. (A) Phase-plane plots of hDRG neurons showing examples from cells with a large shoulder (top) and small shoulder (bottom). Boxed regions indicate the onset and offset of the shoulder, depicted by the slowing rate of membrane voltage change. (B) Histogram showing a distribution of the range of shoulder areas. Inset shows an example action potential waveform and the method used for calculating the shoulder area. Shoulder size was approximated using the formula ½(height × base). (C) Scatter plot of the shoulder areas relative to cell size or current injection threshold. Shoulder areas did not correlate with either measure. Linear fits of the data are shown; $R^2 = 0.013$, $P = .475$ (size); $R^2 = 0.003$, $P = .715$ (rheobase).

studies have never been demonstrated on human sensory neurons. To test whether naïve hDRG neurons respond directly to substances that produce pain and itch, we bath-applied AITC, ATP, histamine, or chloroquine onto a subset of recorded neurons (Fig. 5A–D). Only a single substance was delivered to each neuron. A high proportion of cells (14 of 25, 56%) discharged in response to one of these algogenic or pruritogenic substances, suggesting that hDRG likely possess considerable overlap in their capability to respond to a variety of chemical stimuli.

3.6. Modulation of hDRG excitability by the inflammatory compounds bradykinin and PGE_2

Inflammatory mediators such as bradykinin and prostaglandin E_2 (PGE_2) can activate and sensitize nociceptors from model organisms, but whether hDRG neurons respond directly to these mediators has not been tested. Therefore, we examined ongoing activity and membrane excitability of hDRG neurons exposed to bradykinin. Twenty-seven hDRG neurons were bath-exposed to 100 nM bradykinin, and 13 of these (48%) responded by discharging action potentials (total BK-evoked APs, Table 2). Examples of bradykinin-evoked discharge are in Fig. 6A. In a few cases, cells would undergo spontaneous discharge followed by a return to a quiescent state, with single ectopic action potentials occurring at random times following the initial barrage. To test whether these effects were unique to bradykinin in human DRG, we applied PGE_2 (1 μM) to a subset of naïve neurons and observed similar effects (Fig. 6B). Bradykinin and PGE_2 both enhanced the response to a step current injection with the rheobase often evoking multiple action potentials after exposure (Fig. 6C, D). These findings demonstrate that human sensory neurons can be sensitized by inflammatory mediators; however, we focused our analysis on cells exposed solely to bradykinin to quantify this sensitization.

We first examined the rheobase after bradykinin application and found a significant reduction in the current required to evoke an action potential (Fig. 6E, Table 3). The voltage threshold for initiation of stimulus-evoked action potentials did not change after bradykinin. However, we noticed that after bradykinin, "spontaneous" discharge of action potentials were generated at a significantly more hyperpolarized membrane potential compared to electrically evoked action potentials (Fig. 6F, Table 3). A phase-plane plot of overlapping traces from a single representative neuron before and after exposure to bradykinin is shown in Fig. 6G, illustrating the slower rise time and rates of change in membrane voltage summarized in Table 3. The graph illustrates similar AP thresholds but also shows several bradykinin-induced changes to the action potential waveform, which are described in Table 3. Before bradykinin treatment, step-evoked action potentials were elicited immediately ("start") or were delayed by >10 ms from the onset of the stimulus. Neurons exhibiting this delay were significantly more likely to discharge spontaneously during bradykinin application (78% vs 33%; Table 2; Fisher's exact test, $P < .05$). Interestingly, neurons that discharged spontaneously after bradykinin exhibited significantly longer duration AHPs, measured from step current injections, compared to neurons that did not discharge after bradykinin (mean weighted tau values: depolarize, 16.7 ± 3.7 ms; fire action potential, 45.0±7.2 ms; $n = 14$ and 13, respectively; $P = .0014$; Fig. 6H).

The differences between electrically and chemically evoked action potentials are shown in Table 3. Most notable are the differences in threshold for action potential activation, which was significantly hyperpolarized for bradykinin-induced firing (electrically evoked, −18.1 ± 4.4 mV; bradykinin induced, −45.5 ± 3.8 mV; $n = 11$, paired comparison, $P < .001$). AHP amplitude and tau values were also significantly altered between electrically and chemically evoked AP discharges in the presence of bradykinin. These results confirm that human sensory neurons respond directly to the inflammatory compounds bradykinin and PGE_2 and that exposure can enhance neuronal excitability leading to peripheral sensitization.

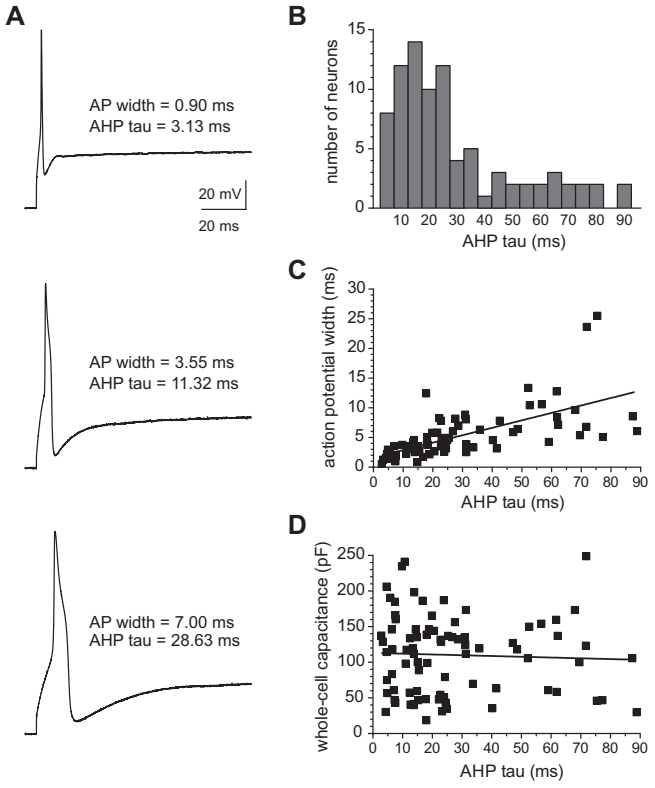

Fig. 4. Human DRG exhibit a wide range of afterhyperpolarization (AHP) decay kinetics that correlate with action potential widths. (A) Example traces of action potentials evoked by step current injections in 3 different human DRG neurons that exhibited markedly different action potential widths and AHP kinetics. (B) Distribution of the mean weighted tau values from fitting the AP AHP from 86 hDRG neurons. Tau values were determined from either single or biexponential fits of the voltage decay. (C, D) Scatter plots showing a strong linear correlation between AHP tau values and action potential widths, but not whole-cell capacitance measurements. Linear fits of the data are shown; $R^2 = 0.432$, $P < .0001$ (C); $R^2 = 0.002$, $P = 0.6989$ (D).

4. Discussion

Clinical trials for pain relief have not replicated many of the findings from studies in animal models, leading to considerable debate on the reasons behind the lack of translational success. Much of the focus has been on the possibility that reflexive behavioral tests of hyperalgesia and sensitization in rodents may not reflect the ongoing nature of human chronic pain [8,34,53]. However, it must not be overlooked that biological differences between model organisms and humans may account for much of the difficulty with translation [16]. Here, we characterized the membrane properties and functional responses to algogens, pruritogens, and inflammatory mediators. Our results show the first demonstrations of activation by itch-producing compounds and membrane sensitization by inflammatory mediators in naïve hDRG neurons.

4.1. Electrophysiology of human sensory neurons

Young adult hDRG neurons in our cultures ranged in diameter from ~30 to 90 μm, consistent with observations from histological sections of whole ganglia and cultures of avulsed ganglia [2,26]. This indicates that our cultures reasonably reflect the total population of hDRG neurons. In rodent models, small-diameter somata (<30 μm) have been linked to slowly conducting axons and are more likely to serve as nociceptors [23,25]. In this study, we focused on the subset of relatively small/medium hDRG neurons between 30 and 60 μm in diameter that are likely to represent the C-fiber and Aδ populations.

Ninety-seven percent of recorded human sensory neurons exhibited a shoulder on the descending phase of the action potential, similar to what has been reported for small-diameter nociceptors from rodents [23,33,39]. These inflections are thought to be the result of a combination of calcium and sodium influx through voltage-gated ion channels and act to prolong AP duration [10]. One consequence of this is increased intracellular calcium in axon terminals, which may enhance neurotransmitter release. Broadened APs in sensory neurons have been correlated with binding of isolectin-B4 (IB4), a marker for nonpeptidergic, small-diameter nociceptors, which possess relatively high thresholds for activation in rodents [22,45]. Given the prolonged shoulder observed in our recordings and the high response rate of tested neurons to various nociceptive stimuli, most small-diameter hDRG neurons are likely to be nociceptors. However, unlike rodent sensory neurons, we found that cultured hDRG neurons do not bind IB4 (unpublished observations), nor did we find that neurons with the largest shoulders correlate with cell size or higher rheobase. Our observation that hDRG do not bind IB4 is consistent with the suggestion that human versican lacks the IB4 binding epitope. Further anatomical and physiological classification of hDRG neurons will, we hope, lead to a clearer delineation of their roles in sensory information processing.

After the inflection, the falling phase of the AP leads to an AHP. A methodological consideration in the present experiments is that AHPs were measured during step current injection, which necessarily interfered with the AHP profile. Nevertheless, a wide range of AHP durations was observed that correlated positively with AP width. Longer-duration AHPs recorded from rodent sensory neurons in vivo have been considered to be an indicator of nociceptors, while shorter AHPs correlate with low threshold mechanoreceptors [11,19,54]. We found that hDRG neurons exhibiting longer duration AHP kinetics in response to electrical stimulation were more likely to fire APs during exposure to bradykinin, suggesting that longer duration AHPs in hDRG neurons are also indicative of nociceptors. We tested the idea that bradykinin could alter AHP kinetics and contribute to sensitization as has been suggested in rodents [29]. Human DRG neurons were resistant to bradykinin-induced changes in AHP amplitude or decay kinetics. The AHP_{slow}, a many-seconds-long AHP evoked by a high-frequency stimulus and inhibited by bradykinin [15,48], was not examined in the present study, but this might serve as a useful parameter for further classification of these neurons.

4.2. Differences between humans and other animals

Among the many differences between humans and most model organisms is the large discrepancy in life spans. For practical reasons, rodent models of persistent and chronic pain are typically measured in the span of days or weeks, whereas human chronic pain conditions are experienced over months and years. In addition to these temporal differences in modeling human pain conditions, distinctions in gene expression and protein function of sensory neurons have been recently identified between humans and other species. For instance, monkey and human DRG neurons express little if any P2X2, an ATP-activated receptor robustly expressed in rodents and involved in rodent models of chronic pain [43]. Additionally, human P2X3 receptors in heterologous cells exhibit greatly reduced antagonist potency relative to P2X3 receptors from nonhuman species [43]. Such functional differences are not limited to purinergic receptors; heterologously expressed human TRPA1 channels exhibited sensitivity to acidic pH. However, both rodent and monkey TRPA1 were insensitive to low pH, highlighting important functional differences even between primate species [13,17]. These examples suggest important evolutionary divergence in the function of hDRG signaling that emphasize the need

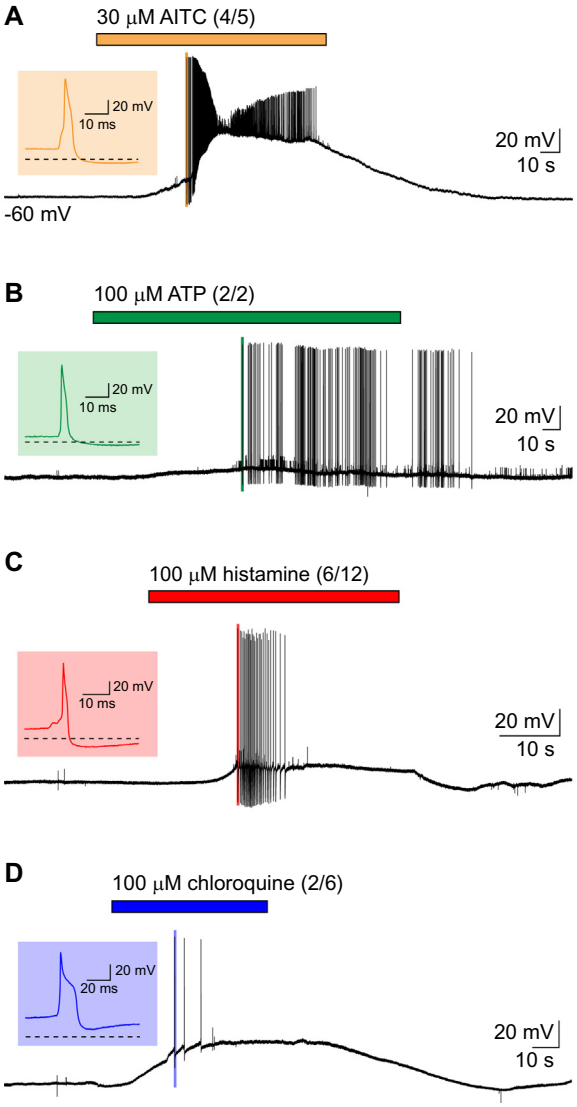

Fig. 5. Human DRGs are activated by chemical algogens and pruritogens. (A–D) Voltage traces depicting responses to AITC (30 μM), ATP (100 μM), histamine (100 μM), and chloroquine (100 μM). Bath application of compounds, indicated by colored rectangles, resulted in action potential discharge in a subset of cells. The number of responsive neurons is indicated in parentheses next to each chemical. The insets depict the AP waveforms of the first action potential in response to chemical application. Dashed lines represent −60 mV.

Table 2
Neuronal responses to BK based on their latency to fire an AP in response to current injection.[a]

AP type	Naïve	BK-evoked APs
Start	18/27 (67%)	6/18 (33%)
Delayed	9/27 (33%)	7/9 (78%)*

AP, action potential; BK, bradykinin.
[a] BK-treated neurons with delayed firing were more likely to spontaneously discharge after treatment. "Start" refers to neurons that fired immediately during step current injections; "delayed" describes neurons that fired >10 ms after a depolarizing pulse. "Naïve" summarizes the proportion of naïve neurons that exhibited either a "start" or "delayed" firing pattern with depolarizing current injection. A significantly higher proportion of neurons with delayed responses to electrical stimulation exhibited BK-evoked firing.
* Statistically significant ($P < .05$, Fisher's exact test).

for continued characterization of receptor and channel properties in human cells. Given the increasing observations documenting the differences between hDRG and those from model organisms, defining the differences between human and model physiology is increasingly important.

4.3. Chemosensitivity

We tested naïve hDRG neurons for sensitivity to several algogens or pruritogens and found a high proportion of chemosensitive cells compared to rodent studies. For example, the TRPA1 receptor, which has been linked to pungent, cold, and mechanical sensation, is activated by the agonist AITC in only about 25% of rodent DRG neurons [4,28,44]. However, we observed responses to AITC in 4 out of 5 hDRG neurons. Similarly, peripheral application of bradykinin elicits acute pain behaviors in both rodents and humans [21,40] and activates 15% to 20% of total mouse DRG in vitro [4,24]. When applied to hDRG neurons, we observed a discharge in 13 of 27 cells (48%). In addition to algogens, we tested the sensitivity of hDRG neurons to the itch-producing compounds histamine and chloroquine. Histamine activated 6 of 12 hDRG neurons in this study, but elicited responses in only ~15% of rodent sensory neurons [24,36]. Similarly, the antimalarial drug chloroquine activates only 4% to 13% of rodent sensory neurons [30,47] but produced responses in 2 out of 6 (33%) hDRG neurons tested. Previous studies of cultured monkey trigeminal neurons likewise showed a high response rate to the algogen capsaicin (9 of 14 cells, 64%) [27], and a similarly large proportion (~65%) of human sensory neurons from ganglionectomized DRG of chronic pain patients were responsive to capsaicin [6,7]. Taken together, these results show a pattern of observations suggesting that humans and nonhuman primates may possess a relatively higher proportion of chemosensitive sensory neurons than rodents. Because of the potential differences in culturing and chemical concentrations between the current study and the wide range of experimental conditions in rodent studies, direct comparisons are difficult and require caution. Further examination of hDRGs using higher-throughput methods such as calcium imaging is needed to clarify the nature of human chemosensitivity.

4.4. Sensitization

Human DRG neurons exposed to bradykinin and PGE_2 exhibited increased discharge to electrical stimulation and lowered rheobase, which outlasted the acute effects of chemical application. In addition, resting membrane potential was depolarized after bradykinin and AP upstroke exhibited slowed kinetics. In rodents, bradykinin-induced sensitization lowers the threshold temperature for heat activation of TRPV1, resulting in enhanced responses to capsaicin and noxious heat [12,14,46,52]. We did not test heat-induced activation in this study; however, our results support the idea that bradykinin-induced sensitization of hDRG neurons may involve functional modulation of membrane excitability. In rodents, PGE_2 sensitizes neurons by lowering the AP threshold and increasing stimulus-evoked discharge by modulating membrane excitability through effects on voltage-gated sodium and potassium channels [23,35]. Further work can determine the nature of the intracellular signaling cascade involved in sensitization of hDRG neurons by these inflammatory mediators.

4.5. Chemically vs electrically evoked action potentials

We observed that hDRG neurons responding to chemical activation produced action potentials with significantly lower AP thresholds than those from current injections. Although current injections typically evoked a single or a few APs, chemically evoked discharge produced multiple action potentials at much higher frequencies. It is possible that current injection into the soma fails to effectively activate the presumed sodium channel-rich areas

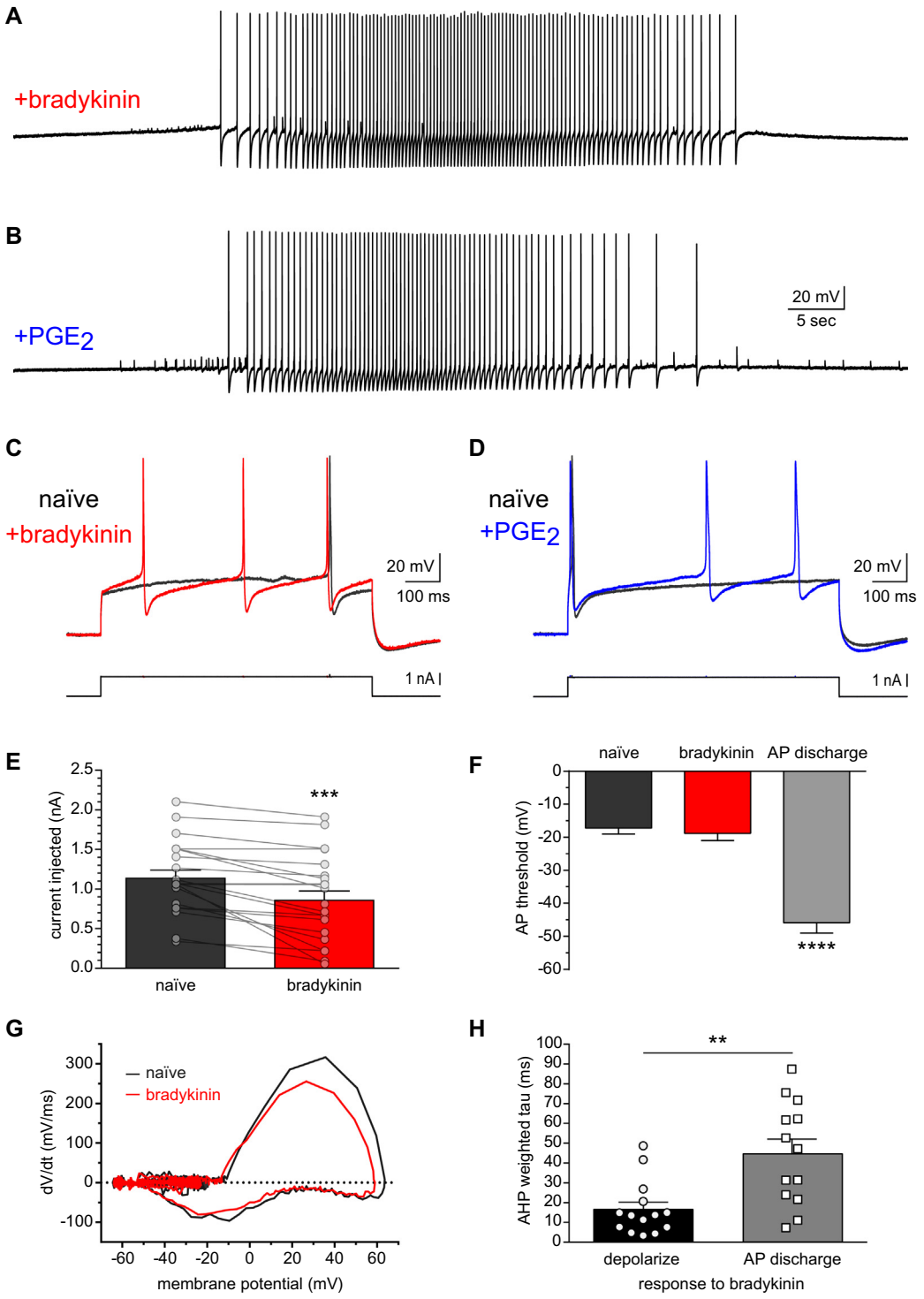

Fig. 6. Human DRG excitability is modulated by the inflammatory compounds bradykinin and PGE_2. (A) Five-minute bath application of bradykinin (100 nM) and (B) prostaglandin E2 (1 μM) produced action potential discharge in a subset of hDRG neurons. These traces are in the continued presence of the indicated inflammatory mediator. (C, D) Voltage traces of action potential firing during threshold step current injections before (black traces) and after exposure to either bradykinin (red) or PGE_2 (blue). Neurons often fired multiple action potentials at rheobase following application of either compound. (E) Summary graph of the injected current threshold to elicit action potentials in neurons before (naïve) and after bradykinin application. Nearly every cell exhibited a lower rheobase after exposure to bradykinin. Paired *t* test, $^{***}P < .001$. (F) Graph of average membrane voltage during electrically evoked action potentials (threshold of 5 mV/ms), before (naïve, dark gray) and after bradykinin (red) exposure. Chemically evoked action potentials had much lower thresholds than those evoked electrically (light gray); $^{****}P < .0001$. (G) Table summarizing the responses to bradykinin (subset of 27 total neurons exposed). Step current-evoked action potentials were delayed (>10 ms) in 33% of hDRG neurons. These delayed-type neurons exhibited significantly greater probability of displaying chemically evoked ongoing activity. Seventy-eight percent of these neurons fired action potentials, whereas only 33% of cells that fired early action potentials exhibited bradykinin-evoked discharge. Fisher's exact test, $P < .05$. (H) Distribution and average AHP tau values for neurons grouped on the basis of their response to bradykinin. Of the 27 cells exposed to bradykinin, 14 experienced transient depolarization without action potential discharge, while the other 13 cells fired action potentials. $^{**}P < .01$.

Table 3
Membrane and action potential parameters, BK sensitization, and comparison of chemical vs electrical excitability.[a]

Parameter	All naïve neurons	BK effect		Electrical vs chemical AP	
		Naïve (evoked)	After BK (evoked)	After BK (evoked)	BK (spontaneous)
Resting potential, mV	−62.36 ± 2.02 (133)	−60.6 ± 1.5 (21)[b]	−58.3 ± 1.9 (21)*,[b]	…	…
Input resistance, MΩ	97.51 ± 10.09 (122)	63.90 ± 13.96 (23)	73.16 ± 20.61 (23)	…	…
Ramp AP, nA	2.45 ± 0.24 (87)	1.96 ± 0.33 (13)[b]	1.56 ± 0.35 (13)***,[b]	…	…
Step rheobase, nA	1.43 ± 0.11 (111)	1.24 ± 0.12 (22)[b]	0.97 ± 0.15 (22)***,[b]	…	…
Threshold, mV	−15.73 ± 1.12 (80)	−16.32 ± 1.70 (24)	−19.02 ± 2.24 (24)	−18.1 ± 4.4 (11)[b]	−45.49 ± 3.77 (11)***,[b]
AP peak, mV	64.64 ± 0.89 (111)	65.89 ± 1.88 (25)	63.03 ± 1.92 (25)	65.04 ± 3.19 (11)	60.53 ± 1.59 (11)
AP rise time, μs	528.4 ± 40.2 (80)	380.4 ± 33.9 (25)[b]	502.9 ± 50.7 (25)**,[b]	552.9 ± 83.6 (11)	536.8 ± 74.2 (11)
AP slope, max, mV/ms	326.9 ± 18.6 (83)	395.2 ± 29.5 (25)[b]	314.4 ± 27.1 (25)*	281.9 ± 37.6 (11)[b]	204.7 ± 6.0 (11)*,[b]
AP slope, min, mV/ms	−100.2 ± 8.6 (83)	−101.6 ± 10.0 (25)	−88.33 ± 9.12 (25)*,[b]	−70.51 ± 13.31 (11)	−71.58 ± 6.83 (11)
AP width, full, ms	4.92 ± 0.42 (79)	5.11 ± 1.05 (24)	4.93 ± 0.69 (24)	6.41 ± 5.69 (12)	5.68 ± 0.74 (12)
AHP amplitude, mV	−52.66 ± 1.21 (52)	−53.66 ± 1.82 (25)	−53.37 ± 1.55 (25)	−51.48 ± 2.52 (12)	−73.07 ± 1.32 (12)***,[b]
AHP kinetics, tau, ms	26.67 ± 2.38 (86)	30.01 ± 5.02 (25)	31.26 ± 4.94 (25)	45.46 ± 6.99 (12)[b]	75.89 ± 10.52 (12)**,[b]

AP, action potential; BK, bradykinin. [a] Data are presented as mean ± standard error of the mean (no. of cells); [b] Significantly different by paired *t* test; * $P < .05$; ** $P < .01$; *** $P < .001$.

within the axon, although our preliminary observations of isolated sodium currents demonstrates evoked currents in the tens of nanoamperes, arguing against this hypothesis. It is possible, however, that the larger size and membrane surface area of hDRG neurons, compared to rDRG, may cause space-clamp issues in these distal processes. Chemical stimulation of these small-diameter axons may therefore be more effective in eliciting localized membrane depolarization. Alternatively, the increased chemical excitability, relative to electrically evoked APs, could be the result of receptor-induced enhancement of voltage-gated ion channels.

Conflict of interest statement

JZ, GP, and AG are paid employees at AnaBios, who provided human DRGs used in these studies. The other authors report no conflict of interest.

Acknowledgments

We thank all members of the Gereau lab for their comments and critiques, and we thank Dr Paul Miller (AnaBios) for assistance in procuring hDRG used in this study as well as his helpful discussion and comments. Supported in part by National Institutes of Health grants NS076324 (SD) and NS042595 (RWG), and a W.M. Keck fellowship (BAC).

References

[1] Anand U, Facer P, Yiangou Y, Sinisi M, Fox M, McCarthy T, Bountra C, Korchev YE, Anand P. Angiotensin II type 2 receptor (AT2 R) localization and antagonist-mediated inhibition of capsaicin responses and neurite outgrowth in human and rat sensory neurons. Eur J Pain 2013;17:1012–26.
[2] Anand U, Otto WR, Casula MA, Day NC, Davis JB, Bountra C, Birch R, Anand P. The effect of neurotrophic factors on morphology, TRPV1 expression and capsaicin responses of cultured human DRG sensory neurons. Neurosci Lett 2006;399:51–6.
[3] Anand U, Otto WR, Sanchez-Herrera D, Facer P, Yiangou Y, Korchev Y, Birch R, Benham C, Bountra C, Chessell IP, Anand P. Cannabinoid receptor CB2 localisation and agonist-mediated inhibition of capsaicin responses in human sensory neurons. PAIN® 2008;138:667–80.
[4] Bandell M, Story GM, Hwang SW, Viswanath V, Eid SR, Petrus MJ, Earley TJ, Patapoutian A. Noxious cold ion channel TRPA1 is activated by pungent compounds and bradykinin. Neuron 2004;41:849–57.
[5] Basbaum AI, Bautista DM, Scherrer G, Julius D. Cellular and molecular mechanisms of pain. Cell 2009;139:267–84.
[6] Baumann TK, Burchiel KJ, Ingram SL, Martenson ME. Responses of adult human dorsal root ganglion neurons in culture to capsaicin and low pH. PAIN® 1996;65:31–8.
[7] Baumann TK, Chaudhary P, Martenson ME. Background potassium channel block and TRPV1 activation contribute to proton depolarization of sensory neurons from humans with neuropathic pain. Eur J Neurosci 2004;19:1343–51.
[8] Bennett GJ. What is spontaneous pain and who has it? J Pain 2012;13:921–9.
[9] Bhave G, Gereau IV RW. Posttranslational mechanisms of peripheral sensitization. J Neurobiol 2004;61:88–106.
[10] Blair NT, Bean BP. Roles of tetrodotoxin (TTX)-sensitive Na^+ current, TTX-resistant Na^+ current, and Ca^{2+} current in the action potentials of nociceptive sensory neurons. J Neurosci 2002;22:10277–90.
[11] Boada MD, Woodbury CJ. Physiological properties of mouse skin sensory neurons recorded intracellularly in vivo: temperature effects on somal membrane properties. J Neurophysiol 2007;98:668–80.
[12] Cesare P, Dekker LV, Sardini A, Parker PJ, McNaughton PA. Specific involvement of PKC-epsilon in sensitization of the neuronal response to painful heat. Neuron 1999;23:617–24.
[13] Chen J, Zhang XF, Kort ME, Huth JR, Sun C, Miesbauer LJ, Cassar SC, Neelands T, Scott VE, Moreland RB, Reilly RM, Hajduk PJ, Kym PR, Hutchins CW, Faltynek CR. Molecular determinants of species-specific activation or blockade of TRPA1 channels. J Neurosci 2008;28:5063–71.
[14] Chuang HH, Prescott ED, Kong H, Shields S, Jordt SE, Basbaum AI, Chao MV, Julius D. Bradykinin and nerve growth factor release the capsaicin receptor from PtdIns(4,5)P2-mediated inhibition. Nature 2001;411:957–62.
[15] Cordoba-Rodriguez R, Moore KA, Kao JP, Weinreich D. Calcium regulation of a slow post-spike hyperpolarization in vagal afferent neurons. Proc Natl Acad Sci USA 1999;96:7650–7.
[16] Craig AD. A rat is not a monkey is not a human: comment on Mogil (Nat Rev Neurosci 2009;10:283–94). Nat Rev Neurosci 2009;10:466.
[17] de la Roche J, Eberhardt MJ, Klinger AB, Stanslowsky N, Wegner F, Koppert W, Reeh PW, Lampert A, Fischer MJ, Leffler A. The molecular basis for species-specific activation of human TRPA1 protein by protons involves poorly conserved residues within transmembrane domains 5 and 6. J Biol Chem 2013;288:20280–92.
[18] Dib-Hajj SD, Tyrrell L, Cummins TR, Black JA, Wood PM, Waxman SG. Two tetrodotoxin-resistant sodium channels in human dorsal root ganglion neurons. FEBS Lett 1999;462:117–20.
[19] Djouhri L, Bleazard L, Lawson SN. Association of somatic action potential shape with sensory receptive properties in guinea-pig dorsal root ganglion neurones. J Physiol 1998;513:857–72.
[20] Dong X, Han S, Zylka MJ, Simon MI, Anderson DJ. A diverse family of GPCRs expressed in specific subsets of nociceptive sensory neurons. Cell 2001;106:619–32.
[21] Dray A, Perkins M. Bradykinin and inflammatory pain. Trends Neurosci 1993;16:99–104.
[22] Fang X, Djouhri L, McMullan S, Berry C, Waxman SG, Okuse K, Lawson SN. Intense isolectin-B4 binding in rat dorsal root ganglion neurons distinguishes C-fiber nociceptors with broad action potentials and high Nav1.9 expression. J Neurosci 2006;26:7281–92.
[23] Gold MS, Dastmalchi S, Levine JD. Co-expression of nociceptor properties in dorsal root ganglion neurons from the adult rat in vitro. Neuroscience 1996;71:265–75.
[24] Han SK, Mancino V, Simon MI. Phospholipase Cbeta 3 mediates the scratching response activated by the histamine H1 receptor on C-fiber nociceptive neurons. Neuron 2006;52:691–703.
[25] Harper AA, Lawson SN. Conduction velocity is related to morphological cell type in rat dorsal root ganglion neurones. J Physiol 1985;359:31–46.
[26] Holford LC, Case P, Lawson SN. Substance P, Neurofilament, peripherin and SSEA4 immunocytochemistry of human dorsal root ganglion neurons obtained from post-mortem tissue: a quantitative morphometric analysis. J Neurocytol 1994;23:577–89.
[27] Ingram SL, Martenson ME, Baumann TK. Responses of cultured adult monkey trigeminal ganglion neurons to capsaicin. NeuroReport 1993;4:460–2.
[28] Jordt SE, Bautista DM, Chuang HH, McKemy DD, Zygmunt PM, Hogestatt ED, Meng ID, Julius D. Mustard oils and cannabinoids excite sensory nerve fibres through the TRP channel ANKTM1. Nature 2004;427:260–5.

[29] Kajekar R, Myers AC. Effect of bradykinin on membrane properties of guinea pig bronchial parasympathetic ganglion neurons. Am J Physiol Lung Cell Mol Physiol 2000;278:L485–91.
[30] Liu Q, Tang Z, Surdenikova L, Kim S, Patel KN, Kim A, Ru F, Guan Y, Weng HJ, Geng Y, Undem BJ, Kollarik M, Chen ZF, Anderson DJ, Dong X. Sensory neuron-specific GPCR Mrgprs are itch receptors mediating chloroquine-induced pruritus. Cell 2009;139:1353–65.
[31] Maddox FN, Valeyev AY, Poth K, Holohean AM, Wood PM, Davidoff RA, Hackman JC, Luetje CW. GABAA receptor subunit mRNA expression in cultured embryonic and adult human dorsal root ganglion neurons. Brain Res Dev 2004;149:143–51.
[32] Martic-Kehl MI, Schibli R, Schubiger PA. Can animal data predict human outcome? Problems and pitfalls of translational animal research. Eur J Nucl Med Mol Imaging 2012;39:1492–6.
[33] McCarthy PW, Lawson SN. Differing action potential shapes in rat dorsal root ganglion neurones related to their substance P and calcitonin gene–related peptide immunoreactivity. J Comp Neurol 1997;388:541–9.
[34] Mogil JS. Animal models of pain: progress and challenges. Nat Rev Neurosci 2009;10:283–94.
[35] Nicol GD, Vasko MR, Evans AR. Prostaglandins suppress an outward potassium current in embryonic rat sensory neurons. J Neurophysiol 1997;77:167–76.
[36] Nicolson TA, Bevan S, Richards CD. Characterisation of the calcium responses to histamine in capsaicin-sensitive and capsaicin-insensitive sensory neurones. Neuroscience 2002;110:329–38.
[37] Nieminen K, Suarez-Isla BA, Rapoport SI. Electrical properties of cultured dorsal root ganglion neurons from normal and trisomy 21 human fetal tissue. Brain Res 1988;474:246–54.
[38] Perel P, Roberts I, Sena E, Wheble P, Briscoe C, Sandercock P, Macleod M, Mignini LE, Jayaram P, Khan KS. Comparison of treatment effects between animal experiments and clinical trials: systematic review. BMJ 2007;334:197.
[39] Ritter AM, Mendell LM. Somal membrane properties of physiologically identified sensory neurons in the rat: effects of nerve growth factor. J Neurophysiol 1992;68:2033–41.
[40] Schmelz M, Schmidt R, Weidner C, Hilliges M, Torebjork HE, Handwerker HO. Chemical response pattern of different classes of C-nociceptors to pruritogens and algogens. J Neurophysiol 2003;89:2441–8.
[41] Scott BS, Petit TL, Becker LE, Edwards BA. Electric membrane properties of human DRG neurons in cell culture and the effect of high K medium. Brain Res 1979;178:529–44.
[42] Seok J, Warren HS, Cuenca AG, Mindrinos MN, Baker HV, Xu W, Richards DR, McDonald-Smith GP, Gao H, Hennessy L, Finnerty CC, Lopez CM, Honari S, Moore EE, Minei JP, Cuschieri J, Bankey PE, Johnson JL, Sperry J, Nathens AB, Billiar TR, West MA, Jeschke MG, Klein MB, Gamelli RL, Gibran NS, Brownstein BH, Miller-Graziano C, Calvano SE, Mason PH, Cobb JP, Rahme LG, Lowry SF, Maier RV, Moldawer LL, Herndon DN, Davis RW, Xiao W, Tompkins RG. Inflammation, host response to injury LSCRP. Genomic responses in mouse models poorly mimic human inflammatory diseases. Proc Natl Acad Sci USA 2013;110:3507–12.
[43] Serrano A, Mo G, Grant R, Pare M, O'Donnell D, Yu XH, Tomaszewski MJ, Perkins MN, Seguela P, Cao CQ. Differential expression and pharmacology of native P2X receptors in rat and primate sensory neurons. J Neurosci 2012;32:11890–6.
[44] Stucky CL, Dubin AE, Jeske NA, Malin SA, McKemy DD, Story GM. Roles of transient receptor potential channels in pain. Brain Res Rev 2009;60:2–23.
[45] Stucky CL, Lewin GR. Isolectin B(4)-positive and -negative nociceptors are functionally distinct. J Neurosci 1999;19:6497–505.
[46] Sugiura T, Tominaga M, Katsuya H, Mizumura K. Bradykinin lowers the threshold temperature for heat activation of vanilloid receptor 1. J Neurophysiol 2002;88:544–8.
[47] Than JY, Li L, Hasan R, Zhang X. Excitation and modulation of TRPA1, TRPV1, and TRPM8 channel-expressing sensory neurons by the pruritogen chloroquine. J Biol Chem 2013;288:12818–27.
[48] Usachev YM, DeMarco SJ, Campbell C, Strehler EE, Thayer SA. Bradykinin and ATP accelerate $Ca^{(2+)}$ efflux from rat sensory neurons via protein kinase C and the plasma membrane $Ca^{(2+)}$ pump isoform 4. Neuron 2002;33:113–22.
[49] Valeyev AY, Hackman JC, Holohean AM, Wood PM, Katz JL, Davidoff RA. GABA-Induced Cl- current in cultured embryonic human dorsal root ganglion neurons. J Neurophysiol 1999;82:1–9.
[50] Valeyev AY, Hackman JC, Wood PM, Davidoff RA. Pharmacologically novel GABA receptor in human dorsal root ganglion neurons. J Neurophysiol 1996;76:3555–8.
[51] van der Worp HB, Howells DW, Sena ES, Porritt MJ, Rewell S, O'Collins V, Macleod MR. Can animal models of disease reliably inform human studies? PLoS Med 2010;7:e1000245.
[52] Vellani V, Mapplebeck S, Moriondo A, Davis JB, McNaughton PA. Protein kinase C activation potentiates gating of the vanilloid receptor VR1 by capsaicin, protons, heat and anandamide. J Physiol 2001;534:813–25.
[53] Vierck CJ, Hansson PT, Yezierski RP. Clinical and pre-clinical pain assessment: are we measuring the same thing? PAIN® 2008;135:7–10.
[54] Waddell PJ, Lawson SN. Electrophysiological properties of subpopulations of rat dorsal root ganglion neurons in vitro. Neuroscience 1990;36:811–22.
[55] White FA, Bhangoo SK, Miller RJ. Chemokines: integrators of pain and inflammation. Nat Rev Drug Discov 2005;4:834–44.
[56] Zylka MJ, Dong X, Southwell AL, Anderson DJ. Atypical expansion in mice of the sensory neuron-specific Mrg G protein-coupled receptor family. Proc Natl Acad Sci USA 2003;100:10043–8.